

Superradiant instability of area quantized Kerr black hole with discrete reflectivity

Zhong-Hao Luo^{1,3,4*} and Yun-Long Zhang^{2,1,5†}

¹*School of Fundamental Physics and Mathematical Sciences,*

Hangzhou Institute for Advanced Study, UCAS, Hangzhou 310024, China.

²*National Astronomy Observatories, Chinese Academy of Science, Beijing, 100101, China*

³*CAS Key Laboratory of Theoretical Physics, Institute of Theoretical Physics,*
Chinese Academy of Sciences, Beijing 100190, China.

⁴*University of Chinese Academy of Sciences, Beijing 100149, China. and*

⁵*International Center for Theoretical Physics Asia-Pacific, Beijing/Hangzhou, China*

(Dated: April 17, 2024)

Ultralight bosons can condense to form the so-called bosonic clouds around spinning black holes by superradiance instability. When quantum effects are taken into account, the classical black holes were replaced by exotic compact objects including area quantized black holes. In this work, we consider the superradiant instabilities of massive scalar fields around area quantized Kerr black hole. We introduce the reflectivity of area quantized black hole possesses the distinct discrete feature, and the scalar fields have the superradiant modes solution only within the specific mass range. In addition, the area quantization may terminate the superradiance when the black hole spins down, or even suppress the formation of the bosonic cloud.

CONTENTS

I. Introduction	1
II. The reflectivity of area quantized black hole	2
A. The discrete energy spectrum	2
B. Transition spectral lines and line width	2
C. Reflectivity with discrete feature	3
III. Axion cloud around area quantized black hole	3
A. The far region solution	4
B. The near region solution	5
C. The overlap region solution	6
IV. Effects on axion clouds from area discretization	7
A. Selection of different superradiant modes	7
B. Termination and suppression of axion clouds	7
V. Conclusion	8
Acknowledgments	8
A. The absorption approximate formula	8
References	9

the corresponding Compton wavelengths of ultralight axions/bosons are about to or larger than the order of black hole scales, the ultralight bosons can be spontaneously amplified to extract the energy and angular momenta of rotating black holes to generate an exponentially growing bosonic cloud. The mechanism is known as superradiant instability [7–12]. This system, so-called gravitational atom [7, 13], is considered to an important gravitational wave source and can be used to constrain parameters of ultralight bosons [14–22].

To resolve the information-loss paradox [23, 24], alternatives to the classical black hole have been proposed to take into account quantum modifications of the theory of gravity near Planck scale of the event horizon, like gravastars [25], boson star [26], and fullball [27]. They commonly are known as exotic compact objects (ECOs). For the classical black holes, due to the causal structure of the geometry, their null surface is a one-way membrane. So classical black holes are perfect absorbers namely possessing a zero reflectivity. But unlike classical black holes, ECOs possess a non-zero reflectivity to result from a surface reflecting the field outwards. One of ECOs, area quantized black hole, absorbs only at selected frequencies. Then the quantum black hole can only undergo transition to discrete energy levels [28].

Area quantized black hole is a phenomenological model proposed by Bekenstein and Mukhanov [29], and has been constructed from first principle approach in loop quantum gravity [30–36]. Any such modification of the boundary condition at the horizon from non-zero reflectivity is expected to affect the response of black hole to external perturbation [37, 38], and due to superradiant instability essentially is a boundary value problem, the reflectivity will affect these axion clouds. In this work, we model the reflectivity of the area-quantized black hole with distinct discrete features. Using an analytic approach in the non-relativistic limit, we investigate massive scalar perturbations with discrete reflectivity. We

I. INTRODUCTION

Ultralight bosons are one of the most well-motivated classes of particles proposed as potential candidates for dark matter, interacting weakly with ordinary matter [1–6]. For their extreme small masses, especially when

* luozhonghao22@mails.ucas.ac.cn

† zhangyunlong@nao.cas.cn

obtain the analytical expression for the growth rates of the axion clouds around area quantized black holes. As a result, we show the influences on the formulation of axion clouds due to the effects of area quantization.

This paper is organized as follows. In Section II, we briefly review the area quantized black hole, and model the reflectivity of them. In Section III, we compute the growth rate of superradiant instability for area-quantized black holes using the reflectivity with distinct discrete feature. In Section IV, we study the selection of different superradiant modes by the axion mass and the termination and suppression of axion clouds. In Section V, we conclude with a discussion and outlook of the results. In this work, we use the $(-, +, +, +)$ convention and take the unit $G = c = 1$.

II. THE REFLECTIVITY OF AREA QUANTIZED BLACK HOLE

Area quantization of the black hole has been introduced by Bekenstein in his pioneering work [39]. Though Christodoulou's work [40], Hawking's area invariance theory [41], it was included that the horizon region of the non-extreme black hole can be regarded as a classical adiabatic invariant. According to Ehrenfest's principle, any classical adiabatic invariant corresponds to a quantum entity with a discrete spectrum. In Christodoulou's work [40], it can be regarded as an adiabatic process when an uncharged particle undergoes the horizon of a black hole at its own radial turning point. The area of this black hole remains invariant as well as the changes of other eliminated parameters.

A. The discrete energy spectrum

In [39], considering Heisenberg's uncertainty principle in the quantum theory, Bekenstein suggested that a classical point particle turns into a particle with an inherent radius. So the area change of the black hole is not zero but a finite value, namely $\Delta A_{\min} = 8\pi\mu b_\mu$, where μ is the mass of this particle, and b_μ is the inherent radius of this particle. If $b_\mu = 0$, then it recovers the classical situation. However, a relativistic particle can not be localized within Compton wavelength, the finite radius of this particle meets $b_\mu \geq \lambda_\mu \equiv \hbar/\mu$. So the minimum area change of a black hole in the quantum theory is $\Delta A_{\min} = 8\pi\ell_P^2$, where $\ell_P = \sqrt{\hbar G/c^3}$ is Planck scale.

When the particle carries an electric charge, the minimum area change is $\Delta A_{\min} = 4\ell_P^2$ [42]. That is to say, for either neutral or charged particles, the limit of the minimum area change is not zero but a finite value considering the uncertainty principle. The difference between them is to consider the vacuum polarization effect of black holes for charged particles, but notably the minimum area changes in both cases are of the same order of magnitude. Thus, due to the quantum effect, black holes

have a uniform discrete area spectrum

$$A = \alpha N \ell_P^2. \quad (1)$$

Here the phenomenological constant $\alpha \in \mathbf{R}$ is a real number depending on concrete physical conditions, and A is the surface area of the black hole.

For the parameters in Kerr black holes, the mass M , the area A and the angular momentum J , meet the following relation

$$M = \sqrt{\frac{A}{16\pi} + \frac{4\pi J^2}{A}}. \quad (2)$$

In [39], Bekenstein assumes that angular momentum can also be quantized

$$J = \hbar j, \quad (0 \leq j \leq \frac{\alpha N}{8\pi}), \quad (3)$$

where j is a semi-integer. Combining it with the above area quantization in Eq. (1), we can get the discrete energy spectrum of the Kerr black hole

$$M_{N,j} = \sqrt{\hbar} \sqrt{\frac{\alpha N}{16\pi} + \frac{4\pi j^2}{\alpha N}}. \quad (4)$$

Compared with classical black hole, the area quantized black hole has an energy gap that prevents some energy from entering the black hole.

B. Transition spectral lines and line width

When a black hole absorbs a perturbation field with the frequency $\omega_{\hat{n}}$ and modes (l, m) on the Kerr background, where l and m are the orbital and azimuthal numbers, $l \geq 0$ and $-l \leq m \leq l$, it will occur to undergo the transition $M_{N,j} \rightarrow M_{N+\Delta N, j+m}$. Thus,

$$\hbar\omega_{\hat{n}} = M_{N+\hat{n}, j+m} - M_{N,j}, \quad (5)$$

where we set $\Delta N = \hat{n}$, and $\omega_{\hat{n}}$ represents the \hat{n} -th absorption spectral line.

When a black hole is a macroscopic black hole, corresponding to the large N limit, the absorption spectra

$$\omega_{\hat{n}} = \frac{\alpha\kappa}{8\pi} \hat{n} + m\Omega_H + O(N^{-1}), \quad (6)$$

where κ and Ω_H are the surface gravity and angular velocity of the Kerr black hole

$$\kappa = \frac{1}{2M} \frac{\sqrt{1-a^2}}{1+\sqrt{1-a^2}}, \quad (7)$$

$$\Omega_H = \frac{1}{2M} \frac{a}{1+\sqrt{1-a^2}}. \quad (8)$$

The dimensionless angular velocity parameter

$$a \equiv J/M^2, \quad 0 \leq a < 1. \quad (9)$$

More detailed derivation can be found in the appendix A.

Considering Hawking radiation of a black hole, the spectral line possesses the width associated with the spontaneous decay of the black hole energy states, just as in atomic physics [43]. In Ref. [44], the analytical fitting function for the line width Γ is found,

$$\Gamma = \frac{1.005}{M} e^{-6.42+1.8a^2+1.9a^{12}-0.1a^{14}}. \quad (10)$$

Thus, since $\Gamma \propto M^{-1}$, the heavier black hole is more stable. And as the spin of the black hole accelerates, the width of absorption spectra also increases.

C. Reflectivity with discrete feature

The perturbation field can be absorbed by the area quantized black hole only at characterized frequencies $f_{\hat{n}} = \omega_{\hat{n}}/2\pi$, while at other frequencies fully reflected. Meanwhile, there is a line width Γ for every transition spectral line. In the frequency range $f_{\hat{n}} - \Gamma/2 < f < f_{\hat{n}} + \Gamma/2$ the reflectivity is zero, and in other frequencies, the reflectivity is one. Thus, the reflectivity \mathcal{R} can be modeled as follow:

$$\mathcal{R} = \begin{cases} 1 - |\Theta(\sin \zeta_1) - \Theta(\sin \zeta_2)|, & \Delta\omega > 2\pi\Gamma \\ 0, & \Delta\omega \leq 2\pi\Gamma \end{cases} \quad (11)$$

where

$$\zeta_1 = \frac{\pi(\omega - m\Omega_H + 2\pi\Gamma/2)}{\Delta\omega}, \quad (12)$$

$$\zeta_2 = \frac{\pi(\omega - m\Omega_H - 2\pi\Gamma/2)}{\Delta\omega}, \quad (13)$$

and $\Theta(\varphi)$ is the unit step function and $\Delta\omega = \alpha\kappa/8\pi$ is the gap of absorption spectra.

Notably, the reflectivity set in Ref. [44] is different from what we set in this work. In Ref. [44], the reflectivity set by them is characterized by pulses, not within the characterized frequency range. It suggests that the reflectivity is not one when the perturbation field absolutely cannot be absorbed by black holes. But the reflectivity should be a constant 1, not within the characterized frequencies range rather than some pulses.

In Fig. 1, we plot the reflectivity \mathcal{R} in Eq. (11) of the area quantized black hole to axions with the superradiant mode $|211\rangle$, which corresponds to the quantum numbers $|nlm\rangle$. Here n is the overtone number, l and m are the orbital and azimuthal numbers. These axions cannot be absorbed by the area-quantized black hole in the low-spin region. As the rotation of the black hole accelerates, the linewidth will continue to increase so that the axions are highly likely to be within the characterized frequency range of the area quantized black hole and to be absorbed. When the linewidth increases to greater than the absorption frequency gap $\Delta\omega = \alpha\kappa/8\pi$,

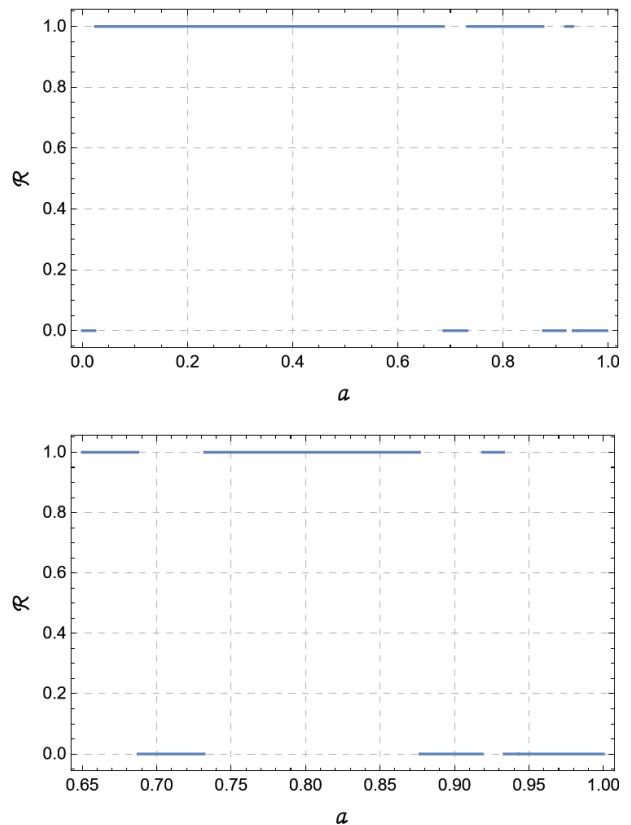


FIG. 1. The reflectivity \mathcal{R} in Eq. (11) of the area quantized black hole with $M = 60M_\odot$ and $\alpha = 8\pi$ has been presented as a function of the dimensionless angular velocity parameter a for the specific mode $|211\rangle$ of the axion mass $\mu = 2.5 \times 10^{-15}$ eV. The bottom figure shows the situation of high spin of the black hole which is highly likely to be absolutely absorbed by the black hole.

the area quantized black hole will recover to the classical black hole with the reflectivity $\mathcal{R} = 0$. And through our calculation, we found only the critical dimensionless spin parameter $a_{\text{crit}} \geq 0.9430$, the absorption spectrum overlaps. It is worth noting that the overlap is not related to the mass of the black hole and external fields from Eq. (6) and Eq. (10). So only the near extreme area quantized black holes can recover to the classical black holes.

III. AXION CLOUD AROUND AREA QUANTIZED BLACK HOLE

In this section, we derive the analytical results of the corrections to the growth rates of superradiant instability. We consider a massive perturbation scalar field around the black hole on the Kerr background with the above discrete reflectivity of the area quantized black hole. We will work in the limit $M/\lambda_\mu = \mu M/\hbar \ll 1$, where μ and M respectively are the mass of the axion and the mass of the black hole.

The metric of the Kerr black hole in Boyer-Linquist

coordinates $\{t, r, \theta, \phi\}$ is

$$\begin{aligned}
ds^2 = & g_{\rho\sigma} dx^\rho dx^\sigma = - \left(1 - \frac{2Mr}{\Sigma}\right) dt^2 + \frac{\Sigma}{\Delta} dr^2 \\
& + \Sigma d\theta^2 - \frac{2Mar \sin^2 \theta}{\Sigma} dt d\phi \\
& + \left(r^2 + a_*^2 + \frac{2Ma_*^2 r}{\Sigma} \sin^2 \theta\right) \sin^2 \theta d\phi^2,
\end{aligned} \tag{14}$$

where M is the black hole mass, and

$$\Sigma = r^2 + a_*^2 \cos^2 \theta, \tag{15}$$

$$\Delta = r^2 - 2Mr + a_*^2 \equiv (r - r_+)(r - r_-). \tag{16}$$

The quantities r_+ and r_- are the radial positions of the outer horizon and the inner horizon, respectively. The angular momentum parameter

$$a_* \equiv J/M = aM. \tag{17}$$

Based on the Kerr background, the massive scalar field ψ obeys the Klein-Gordon equation

$$\nabla^\rho \nabla_\rho \psi = \mu^2 \psi, \tag{18}$$

which can also be written as

$$\frac{1}{\sqrt{-g}} \frac{\partial}{\partial x^\rho} \left(\sqrt{-g} g^{\rho\sigma} \frac{\partial \psi}{\partial x^\sigma} \right) = \mu^2 \psi. \tag{19}$$

where g is the determinant of the Kerr metric $g_{\rho\sigma}$ in (14), and $g^{\rho\sigma}$ is the inverse metric.

Because of the axial symmetry of the Kerr geometry, the field equation can be separable through the ansatz

$$\psi = e^{-i\omega t + im\phi} S(\theta) R(r). \tag{20}$$

We can get two separate equations for the angular function $S(\theta)$,

$$\begin{aligned}
\frac{1}{\sin \theta} \frac{d}{d\theta} \left(\sin \theta \frac{dS}{d\theta} \right) + \left[a_*^2 (\omega^2 - \mu^2) \cos^2 \theta \right. \\
\left. - \frac{m^2}{\sin^2 \theta} + \lambda \right] S = 0,
\end{aligned} \tag{21}$$

and radial function $R(r)$,

$$\begin{aligned}
\Delta \frac{d}{dr} \left(\Delta \frac{dR}{dr} \right) + \left[\omega^2 (r^2 + a_*^2)^2 - 4\omega M r m a_* + m^2 a_*^2 \right. \\
\left. - \Delta (\mu^2 r^2 + a_*^2 \omega^2 + \lambda) \right] R = 0.
\end{aligned} \tag{22}$$

Here λ is the separation constant and can be determined by Eq. (21) as an eigenvalue of it. Meanwhile, the eigenfunctions $S(\theta)$ are the spheroidal harmonics. Notably, λ is not expressible in analytic form in terms of l and n , and it has an approximate expansion form $l(l+1) + O[a^2(\mu^2 - \omega^2)]$. So if $\omega M \ll 1$ and $\mu M \ll 1$ [9],

then the spheroidal harmonics $S(\theta)$ became the spherical harmonics $Y_l^m(\theta)$ and the separation constant

$$\lambda \simeq l(l+1). \tag{23}$$

The angular part $S(\theta)$ of the solution (20) can be approximated as the well-known spherical harmonics in the above limit. So the key to determining the solution is to solve the radial equation (22). The radial perturbation equation can be solved by the matched asymptotic expansion [45]. Namely, one divides the radial part into the far region and the near region.

A. The far region solution

In the far region, where the influence from the black hole can be ignored, the equation can be approximated to a Schrödinger-like equation with a Newtonian potential. In the far region limit, $r \gg M$ and $r \sim l/\omega$, the terms in the radial equation can be approximated as

$$\frac{\Delta \omega^2 a_*^2}{r^4} \sim 0, \quad \frac{\omega M m a_*}{r^3} \sim 0, \quad \frac{m^2 a_*^2}{r^4} \sim 0, \tag{24}$$

$$\frac{\omega^2 (a_*^2 + r^2)^2}{r^4} \simeq \omega^2, \quad \frac{\Delta \mu^2 r^2}{r^4} \simeq \mu^2 \left(1 - \frac{2M}{r}\right), \tag{25}$$

$$\frac{\Delta \frac{d}{dr} \left(\Delta \frac{dR}{dr} \right)}{r^4} \simeq \frac{d^2 R}{dr^2} + \frac{2}{r} \frac{dR}{dr}, \quad \frac{\Delta l(l+1)}{r^4} \simeq \frac{l(l+1)}{r^2}. \tag{26}$$

Then the radial equation (22) can be approximated to the radial hydrogen atom like equation

$$\frac{d^2 (rR)}{dr^2} + \left[\omega^2 - \mu^2 \left(1 - \frac{2M}{r}\right) - \frac{l(l+1)}{r^2} \right] (rR) = 0. \tag{27}$$

After setting $\rho = 2kr$, we obtain

$$\frac{d^2 (\rho R)}{d\rho^2} + \left[-\frac{1}{4} + \frac{\nu}{\rho} - \frac{l(l+1)}{\rho^2} \right] (\rho R) = 0, \tag{28}$$

where the notations

$$k \equiv \sqrt{\mu^2 - \omega^2}, \quad \nu \equiv M\mu^2/k. \tag{29}$$

The solution of Eq. (28) is $\rho R(\rho) = e^{-\rho/2} \rho^{l+1} F(l+1-\nu, 2l+2; \rho)$, namely

$$R(r) = (2kr)^l e^{-kr} F(l+1-\nu, 2l+2; 2kr), \tag{30}$$

where $F(l+1-\nu, 2l+2; 2kr)$ is the confluent hypergeometric function.

Unlike the boundary condition of the electron wave function in the hydrogen atom, which is located at the origin, here the inner boundary condition of this problem is located at the event horizon which corresponds to absorption by the black hole. So the eigenvalues ω should be the complex formula and have corresponding complex ν [46], which satisfy

$$\nu = \nu_0 + \delta\nu, \quad \nu_0 \equiv n+l+1, \tag{31}$$

where $\delta\nu$ is a small complex correction. Then, the solution in Eq. (30) also can be expressed as

$$R(r) = (2kr)^l e^{-kr} F(-n - \delta\nu, 2l + 2; 2kr). \quad (32)$$

B. The near region solution

In the near region, namely the region close to the event horizon, the solution contains the information about the event horizon of the black hole. Because $r = r_+$ is the singularity of the radial equation, as r close to the event horizon, the function R in radial equation (22) varies very rapidly. It is convenient to introduce the rescaled radial coordinate to accommodate this rapid change

$$z \equiv \frac{r - r_+}{r_+ - r_-}, \quad \Delta = z(z + 1)(r_+ - r_-)^2. \quad (33)$$

When $r \ll l/\omega$ or $r \ll l/\mu$, namely $z \ll l/\omega(r_+ - r_-)$ or $z \ll l/\mu(r_+ - r_-)$, then

$$\begin{aligned} \Delta\mu^2 r^2 &= z(z + 1)\mu^2 r^2 / (r_+ - r_-) \ll \Delta l(l + 1), \\ \Delta a_*^2 \omega^2 &= z(z + 1)\omega^2 a_*^2 / (r_+ - r_-) \ll \Delta l(l + 1). \end{aligned} \quad (34)$$

So in Eq. (22), the term

$$\Delta(\mu^2 r^2 + a_*^2 \omega^2 + \lambda) \simeq \Delta\lambda \simeq \Delta l(l + 1). \quad (35)$$

Meanwhile, in the near region,

$$4\omega Mr m a_* \simeq 4\omega Mr_+ m a_*, \quad (36)$$

and

$$\omega^2(r^2 + a_*^2)^2 \simeq \omega^2(r_+^2 + a_*^2)^2 = (2\omega Mr_+)^2, \quad (37)$$

we get

$$\omega^2(r^2 + a_*^2)^2 - 4\omega Mr m a_* + m^2 a_*^2 \simeq (m a_* - 2\omega Mr_+)^2. \quad (38)$$

Then the radial equation in (22) can be approximated as

$$z(z + 1) \frac{d}{dz} \left[z(z + 1) \frac{dR}{dz} \right] + [p^2 - l(l + 1)z(z + 1)]R = 0, \quad (39)$$

where the dimensionless quantity

$$p \equiv \frac{m a_* - 2\omega Mr_+}{r_+ - r_-}. \quad (40)$$

In this differential equation (39), there are three regular singularities $\{0, -1, \infty\}$. We can determine the Riemann P form of the solutions of Eq. (39) by their index equations

$$x_n(x_n - 1) + A_n + B_n = 0, \quad (41)$$

where x_n is the index of linear independent series solutions. A_n is the first order characteristic coefficient and

B_n is the second order characteristic coefficient for n -th singularity. Substituting

$$\begin{aligned} A_0 &= 1, & B_0 &= p^2, \\ A_{-1} &= 1, & B_{-1} &= p^2, \\ A_\infty &= 0, & B_\infty &= -l(l + 1), \end{aligned} \quad (42)$$

we can get the indexes

$$\begin{aligned} x_0^\pm &= \pm ip, & x_{-1}^\pm &= \pm ip, \\ x_\infty^+ &= l + 1, & x_\infty^- &= -l. \end{aligned} \quad (43)$$

So the solution of Eq. (39) is

$$R(z) = P \left\{ \begin{matrix} 0 & -1 & \infty \\ ip & -ip & -l \\ -ip & ip & l + 1 \end{matrix} ; z \right\} \quad (44)$$

$$= \left(\frac{z}{z + 1} \right)^{ip} P \left\{ \begin{matrix} 1 & 0 & \infty \\ 0 & 0 & -l \\ -2ip & 2ip & l + 1 \end{matrix} ; z + 1 \right\} \quad (45)$$

$$= \left(\frac{z}{z + 1} \right)^{ip} F(-l, l + 1, 1 - 2ip; z + 1), \quad (46)$$

where Eq. (44) is the *Riemann P equation* [47].

The hypergeometry function $F(-l, l + 1, 1 - 2ip; z + 1)$ can be expressed by two linear independent solutions,

$$\begin{aligned} &F(-l, l + 1, 1 - 2ip; z + 1) \\ &= P \left\{ \begin{matrix} 1 & 0 & \infty \\ 0 & 0 & -l \\ -2ip & 2ip & l + 1 \end{matrix} ; z + 1 \right\} \\ &= (-z^{-1})^{-l} P \left\{ \begin{matrix} \infty & 1 & 0 \\ -l & 0 & 0 \\ -l - 2ip & 2ip & 2l + 1 \end{matrix} ; -z^{-1} \right\} \\ &= (-z)^l F(-l, -l - 2ip, -2l, -z^{-1}) \equiv U_3, \end{aligned} \quad (47)$$

and

$$\begin{aligned} &F(-l, l + 1, 1 - 2ip; z + 1) \\ &= P \left\{ \begin{matrix} 1 & 0 & \infty \\ 0 & 0 & -l \\ -2ip & 2ip & l + 1 \end{matrix} ; z + 1 \right\} \\ &= (-z^{-1})^{l+1} P \left\{ \begin{matrix} \infty & 1 & 0 \\ l + 1 & 0 & -2l - 1 \\ l + 1 - 2ip & 2ip & 0 \end{matrix} ; -z^{-1} \right\} \\ &= (-z)^{-l-1} F(l + 1, l + 1 - 2ip, 2l + 2, -z^{-1}) \equiv U_4. \end{aligned} \quad (48)$$

So the solution of Eq. (39) can be expressed as follows,

$$R(z) = \left(\frac{z}{z + 1} \right)^{ip} F(-l, l + 1, 1 - 2ip; z + 1) \quad (49)$$

$$= A \left(\frac{z}{z + 1} \right)^{ip} U_3 + B \left(\frac{z}{z + 1} \right)^{ip} U_4, \quad (50)$$

where A and B are the expansion coefficient of U_3 and U_4 respectively.

U_3 and U_4 cannot be represented as the ingoing and outgoing solutions, but two other linear combinations of them U_1 and U_5 can,

$$(U_3, U_4) = (U_1, U_5) \begin{pmatrix} f_{13} & f_{14} \\ f_{53} & f_{54} \end{pmatrix}, \quad (51)$$

where

$$U_1 = {}_2F_1(-l, l+1, 1+2ip; -z), \quad (52)$$

$$U_5 = (-z)^{-2ip} {}_2F_1(-l-2ip, l+1-2ip, 1-2ip; -z), \quad (53)$$

and

$$f_{13} = (-1)^l \frac{\Gamma(-2l)\Gamma(-2ip)}{\Gamma(-l)\Gamma(-2ip-l)}, \quad (54)$$

$$f_{53} = (-1)^l \frac{\Gamma(-2l)\Gamma(2ip)}{\Gamma(-l+2ip)\Gamma(-l)}, \quad (55)$$

$$f_{14} = (-1)^{1-l} \frac{\Gamma(2l+2)\Gamma(-2ip)}{\Gamma(l+1)\Gamma(l-2ip+1)}, \quad (56)$$

$$f_{54} = (-1)^{1-l} \frac{\Gamma(2l+2)\Gamma(2ip)}{\Gamma(l+1)\Gamma(l+2ip+1)}. \quad (57)$$

Finally, the radial solution of Eq. (39) can be expressed as

$$R(z) = A \left(\frac{z}{z+1} \right)^{ip} U_3 + B \left(\frac{z}{z+1} \right)^{ip} U_4 \quad (58)$$

$$= \left(\frac{z}{z+1} \right)^{ip} (U_1, U_5) \begin{pmatrix} f_{13} & f_{14} \\ f_{53} & f_{54} \end{pmatrix} \begin{pmatrix} A \\ B \end{pmatrix}. \quad (59)$$

Using the boundary condition of the event horizon, the reflectivity is

$$\mathcal{R} = \frac{Af_{53} + Bf_{54}}{Af_{13} + Bf_{14}}. \quad (60)$$

We can get the relation between A and B through the above equation

$$A = B \left(\frac{f_{54} - \mathcal{R}f_{14}}{\mathcal{R}f_{13} - f_{53}} \right). \quad (61)$$

C. The overlap region solution

In the overlap region, we connect the solutions in the near region with the ones in the far region to derive the physical solutions. For the property of confluent hypergeometric functions

$$\begin{aligned} & F(-n - \delta\nu, 2l + 2; 2kr) \\ &= \frac{\Gamma(-2l - 1)}{\Gamma(-n - \delta\nu - 2n - 1)} F(-n - \delta\nu, 2l + 2; 2kr) \\ &+ \frac{(2kr)^{-2l-1} \Gamma(2l+1)}{\Gamma(-n - \delta\nu)} F(-n - \delta\nu - 2l - 1, -2l; 2kr), \end{aligned} \quad (62)$$

and Gamma functions

$$\frac{\Gamma(-2l - 1)}{\Gamma(-n - \delta\nu - 2l - 1)} = (-1)^n \frac{\Gamma(2l + n + 2)}{\Gamma(2l + 2)}, \quad (63)$$

$$\frac{\Gamma(2l + 1)}{\Gamma(-n - \delta\nu)} = (-1)^{n+1} \delta\nu \Gamma(n + 1) \Gamma(2l + 1). \quad (64)$$

So the near asymptotic expansion behavior of the far solutions in the overlap region at $2kr \rightarrow 0$ is

$$\begin{aligned} R(r) &= (2kr)^l e^{-kr} F(-n - \delta\nu, 2l + 2; 2kr) \\ &\simeq (-1)^n \frac{\Gamma(2l + n + 2)}{\Gamma(2l + 2)} (2kr)^{l+} \\ &(-1)^{n+1} \Gamma(n + 1) \Gamma(2l + 1) \delta\nu (2kr)^{-l-1}. \end{aligned} \quad (65)$$

Meanwhile, when $r \gg M$ for

$$U_3 \simeq (-z)^l = \left(\frac{-r}{r_+ - r_-} \right)^l, \quad (66)$$

$$U_4 \simeq (-z)^{-l-1} = \left(\frac{-r}{r_+ - r_-} \right)^{-l-1}, \quad (67)$$

the remote asymptotic behavior the near solutions in the overlap region is

$$R(r) \simeq A \left(\frac{-r}{r_+ - r_-} \right)^l + B \left(\frac{-r}{r_+ - r_-} \right)^{-l-1}. \quad (68)$$

These two solutions, Eq. (65) and Eq. (68), can be matched to determine A and B in the overlap region. Considering the relation between A and B in Eq. (61), we can derive the formula of $\delta\nu$

$$\begin{aligned} \delta\nu &= \frac{[2k(r_+ - r_-)]^{2l+1} \Gamma(-2l) \Gamma(l+1) (\Gamma(2l+n+2))}{\Gamma(-l) \Gamma(2l+1) \Gamma(2l+2)^2 \Gamma(n+1)} \\ &\times \frac{\Gamma(l-2ip+1) \Gamma(l+2ip+1)}{\Gamma(2ip-l) \Gamma(-l-2ip)} \\ &\times \frac{\Gamma(2ip) \Gamma(-l-2ip) - \mathcal{R} \Gamma(-2ip) \Gamma(2ip-l)}{\Gamma(2ip) \Gamma(l-2ip+1) - \mathcal{R} \Gamma(-2ip) \Gamma(l+2ip+1)} \\ &= \frac{[2k(r_+ - r_-)]^{2l+1} \Gamma(l) \Gamma(l+1) (\Gamma(2l+n+2))}{\Gamma(2l) \Gamma(2l+1) \Gamma(2l+2)^2 \Gamma(n+1)} \\ &\times 2ip \prod_{j=1}^l (j^2 + 4p^2) \frac{1 - \mathcal{R} \prod_{j=1}^l \frac{j-2ip}{j+2ip}}{1 + \mathcal{R} \prod_{j=1}^l \frac{j-2ip}{j+2ip}}. \end{aligned} \quad (69)$$

Considering $\delta\nu \ll 1$, with $k^2 \equiv \mu^2 - \omega^2$ and $\nu \equiv M\mu^2/k = \nu_0 + \delta\nu$, the eigen-frequency ω is solved as

$$\omega = \mu \left[1 - \left(\frac{M\mu}{\nu_0 + \delta\nu} \right)^2 \right]^{1/2} \simeq \omega_0 + \delta\omega, \quad (70)$$

where $\nu_0 = l + n + 1$ and

$$\begin{aligned} \omega_0 &= \mu \left[1 - \left(\frac{\varepsilon}{\nu_0} \right)^2 \right]^{1/2}, \\ \delta\omega &= \frac{\delta\nu}{M} \left(\frac{\varepsilon}{\nu_0} \right)^3 \left[1 - \left(\frac{\varepsilon}{\nu_0} \right)^2 \right]^{-1/2}. \end{aligned} \quad (71)$$

The gravitational coupling constant has been introduced

$$\varepsilon \equiv M\mu. \quad (72)$$

So we can see when the reflectivity of the black hole is not zero, the growing rate of this scalar cloud is

$$\text{Im}[\delta\omega] = \frac{\delta\nu_*}{M} \left(\frac{\varepsilon}{\nu_0}\right)^3 \left[1 - \left(\frac{\varepsilon}{\nu_0}\right)^2\right]^{-1/2} \times \frac{1 - \mathcal{R}^2}{1 + \mathcal{R}^2 + 2\mathcal{R} \cos(i \sum_{j=1}^l \ln \frac{j+2ip}{j-2ip})}, \quad (73)$$

where

$$\delta\nu_* = \frac{2p}{n!} \left[\frac{l!}{(2l)!(2l+1)!} \right]^2 \prod_{j=1}^l (j^2 + 4p^2) \times (2l+n+1)! [2k(r_+ - r_-)]^{2l+1}. \quad (74)$$

Notice that we use another set of hypergeometry function bases which are different from [48], but get a similar result. One difference is that an additional correction factor $[1 - (\varepsilon/\nu_0)^2]^{-1/2}$ is kept here.

IV. EFFECTS ON AXION CLOUDS FROM AREA DISCRETIZATION

In this section, we consider the growing rates of the different superradiant modes $|nlm\rangle$ from area quantization. For black holes with specific spin and mass, the axions will select the superradiant modes within different mass ranges. Meanwhile, for axions possessing a certain mass, the superradiant modes may be suppressed for black holes with low spins, and recover from discrete to continuous as the spin of black holes increases. Besides, area discretization can also cause the termination of axion clouds.

A. Selection of different superradiant modes

In Fig. 2, we plot the superradiance growth rates $\omega_I \equiv \text{Im}[\delta\omega]$ in Eq. (73) of different three fundamental modes $|nlm\rangle$ with different angular momentum parameter a . It is normalised by $\omega_{\text{yr}} \equiv 2\pi/T_{\text{yr}}$, and T_{yr} is the time for one year. For the area quantized black hole with $a = 0.6$ and $M = 60M_\odot$, within the range of axion mass $2.53 \times 10^{-13}\text{eV} \leq \mu \leq 3.03 \times 10^{-13}\text{eV}$ ($0.1013 \leq \varepsilon \leq 0.1210$), there is only the $|322\rangle$ mode (solid orange curve) and other two modes $|211\rangle$ (light blue curve) and $|321\rangle$ (light green curve) are suppressed. While within the range of axion mass $3.93 \times 10^{-13}\text{eV} \leq \mu \leq 4.42 \times 10^{-13}\text{eV}$ ($0.1570 \leq \varepsilon \leq 0.1767$), the modes $|211\rangle$ and $|321\rangle$ exist but the mode $|322\rangle$ not. In other regions, such as within the range of axion mass $3.03 \times 10^{-13}\text{eV} \leq \mu \leq 3.92 \times 10^{-13}\text{eV}$ ($0.1210 < \varepsilon < 0.1569$), three superradiant modes all are suppressed, while the three modes all

exit for the classical black hole. And within the range of axion mass $8.11 \times 10^{-13}\text{eV} \leq \mu \leq 8.60 \times 10^{-13}\text{eV}$ ($0.3244 < \varepsilon < 0.3443$), there is only the mode $|322\rangle$ in line with the case of the classical black hole.

Compared with the case of $a = 0.6$, in the case of $a = 0.7$ the mode $|322\rangle$ (brown curve) is in the range of larger axion mass in the low ε region, since the absorption spectra Eq. (6) increases as the spin of the black hole accelerates. It leads more overlapping range of axion mass for three modes in line with the case of the classical black hole.

Due to the existence of energy gaps of area quantized black hole, some superradiant modes may be suppressed for the axion with a certain mass. And the selection of the modes varies for axion within different mass ranges.

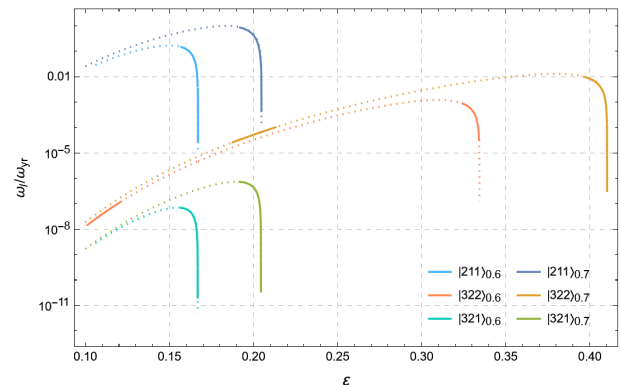


FIG. 2. We plot the superradiance growth rates $\omega_I/\omega_{\text{yr}}$ in Eq. (73) of different three fundamental modes as a function of ε for two black hole spin parameters $a = 0.6$ and $a = 0.7$, where $\omega_I \equiv \text{Im}[\delta\omega]$ and $\omega_{\text{yr}} \equiv 2\pi/T_{\text{yr}}$. The dotted curves represent growth rates for classical black holes and the solid curves represent one for area quantized black hole.

B. Termination and suppression of axion clouds

If the black hole is the area quantized, the clouds of the domain modes are unlikely to form for low-spin black holes. Because the width of the absorption spectral is not large enough for low-spin black holes, the reflectivity typically is one for the axions. As the spin of the black holes increases, the area quantized black holes are more like the classical black holes for the specific mode field. So for a high-spin black hole, the spectrum likely recovers the continues.

In Fig. 3, for the quantized black holes black holes with $M = 60M_\odot$ and $0.3 \lesssim a \lesssim 0.4$, the three domain modes $|211\rangle$, $|322\rangle$ and $|321\rangle$ are absent. So area discretization of the black hole is one of the factors preventing axion cloud formation. On the other hand, the axion cloud may terminate as it spins down the area quantized black hole. For example, for $|211\rangle$ mode in Fig. 3, the axion cloud forms around the black hole with $a = 0.732$. As the axion cloud spins down the black hole, the growing rate

of the mode becomes zero until the spin of the black hole drops to $a = 0.687$ and the axion clouds will terminate.

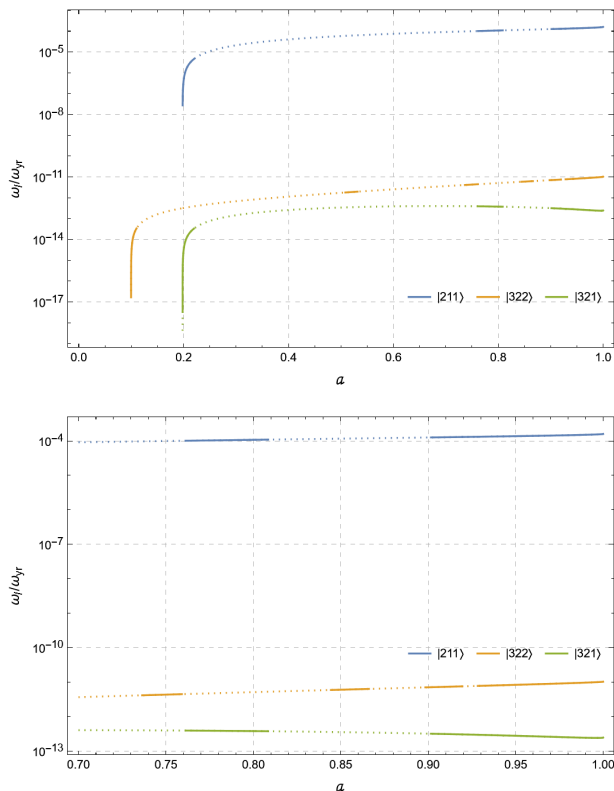


FIG. 3. We have plotted the growth rates ω_I/ω_{yr} of the fundamental modes $|211\rangle$, $|322\rangle$ and $|321\rangle$ as a function of the spin parameter a of the area quantized black hole with $M = 60M_\odot$ in the low-frequency ($\varepsilon = 0.05 \ll 1$) regime. The bottom plot indicates that the growth rates recover to the classical continuous situation as the spin of the black hole increases. The dotted curves represent growth rates for classical black holes and the solid curves represent that for area quantized ones.

V. CONCLUSION

Based on Bekenstein and Mukhanov's proposal [29], the area-quantized black hole possesses non-zero and discrete reflectivity. The non-zero reflectivity will affect the growing rates of superradiant instability, bringing multiple effects to the formulation of axion clouds. In this work, we model the reflectivity of the area quantized Kerr black hole for the massive scalar field. Analytically, we derive the corrective growth rates by solving the massive scalar field perturbation equation on the Kerr background with the above discrete reflectivity. We find that within the different ranges of the axion mass, the axion clouds will have different superradiant states.

Besides, we demonstrate that the area discretization of the black hole may be one of the factors preventing axion clouds formation. Meanwhile, the suppression and termination for the formation of axion clouds can also

distinguish area-quantized black holes from other models of horizonless compact objects. The axion clouds surrounding the black holes can radiate gravitational waves or even the fast radio bursts [49, 50], which provides interesting gravitational phenomenology of astronomical observations [51, 52]. In the following work, we hope to study these effects of area quantization to effectively probe those astrophysical black hole systems.

ACKNOWLEDGMENTS

This work is supported by the National Natural Science Foundation of China under Grant No.12375059 and the Fundamental Research Funds for the Central Universities.

Appendix A: The absorption approximate formula

Here we derive the absorption approximate formula in Eq. (6) under large N limit. Approximately, Eq. (4) can be expanded as

$$\begin{aligned} M_{N+\Delta N, j+\Delta j} &= \sqrt{\hbar} \sqrt{\frac{\alpha(N+\Delta N)}{16\pi} + \frac{4\pi(j+\Delta j)^2}{\alpha(N+\Delta N)}} \\ &\simeq M_{N,j} + \frac{\partial M_{N,j}}{\partial N} \Delta N + \frac{\partial M_{N,j}}{\partial j} \Delta j + O\left(\frac{\Delta N}{N}, \frac{\Delta j}{j}\right). \end{aligned} \quad (\text{A1})$$

Substituting the above equation into Eq. (5), we get

$$\begin{aligned} M_{N+\Delta N, j+\Delta j} - M_{N,j} &\simeq \frac{\partial M_{N,j}}{\partial N} \Delta N + \frac{\partial M_{N,j}}{\partial j} \Delta j \\ &= \frac{1}{2M} \left(\frac{\hbar\alpha}{16\pi} - \frac{4\pi\hbar j^2}{\alpha N^2} \right) \Delta N + \frac{1}{2M} \left(\frac{8\pi\hbar j}{\alpha N} \right) \Delta j. \end{aligned} \quad (\text{A2})$$

Consider the following relations

$$A = 8\pi M^2(1 + \sqrt{1-a^2}), \quad (\text{A3})$$

$$j = \frac{aM^2}{\hbar}, \quad (0 \leq j \leq \frac{\alpha N}{8\pi}), \quad (\text{A4})$$

$$N = A/\hbar\alpha, \quad (\text{A5})$$

the first term in Eq. (A2) becomes

$$\frac{1}{2M} \left(\frac{\hbar\alpha}{16\pi} - \frac{4\pi\hbar j^2}{\alpha N^2} \right) = \frac{\hbar\alpha}{16\pi M} \frac{\sqrt{1-a^2}}{1+\sqrt{1-a^2}} = \frac{\hbar\alpha\kappa}{8\pi}, \quad (\text{A6})$$

where $\kappa \equiv \frac{1}{2M} \frac{\sqrt{1-a^2}}{1+\sqrt{1-a^2}}$ is the surface gravitation of the Kerr black hole. The second term in Eq. (A2) becomes

$$\frac{1}{2M} \left(\frac{8\pi\hbar j}{\alpha N} \right) = \frac{\hbar a}{2M(1+\sqrt{1-a^2})} = \hbar\Omega_H, \quad (\text{A7})$$

where $\Omega_H \equiv \frac{1}{2M} \frac{a}{1+\sqrt{1-a^2}}$ is the surface angular velocity of the Kerr black hole.

So with $\Delta N = \hat{n}$, $\Delta j = m$, we can get

$$\begin{aligned} \hbar\omega_{\hat{n}} &\simeq \frac{\partial M_{N,j}}{\partial N} \Delta N + \frac{\partial M_{N,j}}{\partial j} \Delta j + O\left(\frac{\Delta N}{N}, \frac{\Delta j}{j}\right) \\ &\simeq \hbar\hat{n} \frac{\alpha\kappa}{8\pi} + \hbar m \Omega_H + O(N^{-1}). \end{aligned} \quad (\text{A8})$$

Furthermore, due to the correspondence principle, the approximate expansion also indeed satisfies the macroscopic first law of Kerr black hole

$$dM = \frac{\kappa}{8\pi} dA + \Omega_H dJ = \hbar\hat{n} \frac{\kappa\alpha}{8\pi} + \hbar m \Omega_H, \quad (\text{A9})$$

which is consistent with (A8) considering $dM = \hbar\omega_{\hat{n}}$.

-
- [1] A. Berlin, N. Blinov, G. Krnjaic, P. Schuster, and N. Toro, Dark Matter, Millicharges, Axion and Scalar Particles, Gauge Bosons, and Other New Physics with LDMX, *Phys. Rev. D* **99**, 075001 (2019), arXiv:1807.01730 [hep-ph].
- [2] A. Arvanitaki, S. Dimopoulos, S. Dubovsky, N. Kaloper, and J. March-Russell, String Axiverse, *Phys. Rev. D* **81**, 123530 (2010), arXiv:0905.4720 [hep-th].
- [3] I. G. Irastorza and J. Redondo, New experimental approaches in the search for axion-like particles, *Prog. Part. Nucl. Phys.* **102**, 89 (2018), arXiv:1801.08127 [hep-ph].
- [4] G. Arcadi, M. Dutra, P. Ghosh, M. Lindner, Y. Mambrini, M. Pierre, S. Profumo, and F. S. Queiroz, The waning of the WIMP? A review of models, searches, and constraints, *Eur. Phys. J. C* **78**, 203 (2018), arXiv:1703.07364 [hep-ph].
- [5] M. Schumann, Direct Detection of WIMP Dark Matter: Concepts and Status, *J. Phys. G* **46**, 103003 (2019), arXiv:1903.03026 [astro-ph.CO].
- [6] J. M. Gaskins, A review of indirect searches for particle dark matter, *Contemp. Phys.* **57**, 496 (2016), arXiv:1604.00014 [astro-ph.HE].
- [7] D. Baumann, H. S. Chia, J. Stout, and L. ter Haar, The Spectra of Gravitational Atoms, *JCAP* **12**, 006, arXiv:1908.10370 [gr-qc].
- [8] S. Detweiler, Klein-gordon equation and rotating black holes, *Phys. Rev. D* **22**, 2323 (1980).
- [9] A. A. Starobinskii, Amplification of waves during reflection from a rotating, *Journal of Experimental and Theoretical Physics* (1973).
- [10] R. Brito, V. Cardoso, and P. Pani, Superradiance: New Frontiers in Black Hole Physics, *Lect. Notes Phys.* **906**, pp.1 (2015), arXiv:1501.06570 [gr-qc].
- [11] O. J. C. Dias, G. Lingetti, P. Pani, and J. E. Santos, Black hole superradiant instability for massive spin-2 fields, *Phys. Rev. D* **108**, L041502 (2023), arXiv:2304.01265 [gr-qc].
- [12] P. Pani, V. Cardoso, L. Gualtieri, E. Berti, and A. Ishibashi, Perturbations of slowly rotating black holes: Massive vector fields in the kerr metric, *Phys. Rev. D* **86**, 104017 (2012).
- [13] D. Baumann, H. S. Chia, R. A. Porto, and J. Stout, Gravitational Collider Physics, *Phys. Rev. D* **101**, 083019 (2020), arXiv:1912.04932 [gr-qc].
- [14] R. Brito, V. Cardoso, and P. Pani, Black holes as particle detectors: evolution of superradiant instabilities, *Class. Quant. Grav.* **32**, 134001 (2015), arXiv:1411.0686 [gr-qc].
- [15] R. Brito, S. Ghosh, E. Barausse, E. Berti, V. Cardoso, I. Dvorkin, A. Klein, and P. Pani, Stochastic and resolvable gravitational waves from ultralight bosons, *Phys. Rev. Lett.* **119**, 131101 (2017), arXiv:1706.05097 [gr-qc].
- [16] A. Arvanitaki, M. Baryakhtar, S. Dimopoulos, S. Dubovsky, and R. Lasenby, Black hole mergers and the qcd axion at advanced ligo, *Phys. Rev. D* **95**, 043001 (2017).
- [17] L. Tsukada, T. Callister, A. Matas, and P. Meyers, First search for a stochastic gravitational-wave background from ultralight bosons, *Phys. Rev. D* **99**, 103015 (2019), arXiv:1812.09622 [astro-ph.HE].
- [18] J. Zhang and H. Yang, Dynamic Signatures of Black Hole Binaries with Superradiant Clouds, *Phys. Rev. D* **101**, 043020 (2020), arXiv:1907.13582 [gr-qc].
- [19] S. J. Zhu, M. Baryakhtar, M. A. Papa, D. Tsuna, N. Kawanaka, and H.-B. Eggenstein, Characterizing the continuous gravitational-wave signal from boson clouds around Galactic isolated black holes, *Phys. Rev. D* **102**, 063020 (2020), arXiv:2003.03359 [gr-qc].
- [20] S. Sun and Y.-L. Zhang, Fast gravitational wave bursts from axion clumps, *Phys. Rev. D* **104**, 103009 (2021), arXiv:2003.10527 [hep-ph].
- [21] L. Tsukada, R. Brito, W. E. East, and N. Siemonsen, Modeling and searching for a stochastic gravitational-wave background from ultralight vector bosons, *Phys. Rev. D* **103**, 083005 (2021), arXiv:2011.06995 [astro-ph.HE].
- [22] J. Yang, N. Xie, and F. P. Huang, Implication of nano-Hertz stochastic gravitational wave background on ultralight axion particles and fuzzy dark matter, (2023), arXiv:2306.17113 [hep-ph].
- [23] A. Almheiri, D. Marolf, J. Polchinski, and J. Sully, Black Holes: Complementarity or Firewalls?, *JHEP* **02**, 062, arXiv:1207.3123 [hep-th].
- [24] J. Polchinski, The Black Hole Information Problem, in *Theoretical Advanced Study Institute in Elementary Particle Physics: New Frontiers in Fields and Strings* (2017) pp. 353–397, arXiv:1609.04036 [hep-th].
- [25] P. O. Mazur and E. Mottola, Gravitational condensate stars: An alternative to black holes, *Universe* **9**, 10.3390/universe9020088 (2023).
- [26] F. E. Schunck and E. W. Mielke, General relativistic boson stars, *Class. Quant. Grav.* **20**, R301 (2003), arXiv:0801.0307 [astro-ph].
- [27] K. Skenderis and M. Taylor, The fuzzball proposal for black holes, *Phys. Rept.* **467**, 117 (2008), arXiv:0804.0552 [hep-th].
- [28] I. Agullo, V. Cardoso, A. D. Rio, M. Maggiore, and J. Pullin, Potential Gravitational Wave Signatures of Quantum Gravity, *Phys. Rev. Lett.* **126**, 041302 (2021), arXiv:2007.13761 [gr-qc].
- [29] J. D. Bekenstein and V. F. Mukhanov, Spectroscopy of the quantum black hole, *Phys. Lett. B* **360**, 7 (1995), arXiv:gr-qc/9505012.
- [30] C. Rovelli and L. Smolin, Discreteness of area and volume in quantum gravity, *Nucl. Phys. B* **442**, 593 (1995),

- [Erratum: Nucl.Phys.B 456, 753–754 (1995)], [arXiv:gr-qc/9411005](#).
- [31] C. Rovelli, Black hole entropy from loop quantum gravity, *Phys. Rev. Lett.* **77**, 3288 (1996), [arXiv:gr-qc/9603063](#).
- [32] A. Ashtekar, J. Baez, A. Corichi, and K. Krasnov, Quantum geometry and black hole entropy, *Phys. Rev. Lett.* **80**, 904 (1998), [arXiv:gr-qc/9710007](#).
- [33] A. Ashtekar, J. C. Baez, and K. Krasnov, Quantum geometry of isolated horizons and black hole entropy, *Adv. Theor. Math. Phys.* **4**, 1 (2000), [arXiv:gr-qc/0005126](#).
- [34] I. Agullo, J. F. Barbero G., J. Diaz-Polo, E. Fernandez-Borja, and E. J. S. Villasenor, Black hole state counting in LQG: A Number theoretical approach, *Phys. Rev. Lett.* **100**, 211301 (2008), [arXiv:0802.4077 \[gr-qc\]](#).
- [35] I. Agullo, J. Fernando Barbero, E. F. Borja, J. Diaz-Polo, and E. J. S. Villasenor, Detailed black hole state counting in loop quantum gravity, *Phys. Rev. D* **82**, 084029 (2010), [arXiv:1101.3660 \[gr-qc\]](#).
- [36] G. J. Fernando Barbero, J. Lewandowski, and E. J. S. Villasenor, Flux-area operator and black hole entropy, *Phys. Rev. D* **80**, 044016 (2009), [arXiv:0905.3465 \[gr-qc\]](#).
- [37] S. A. Teukolsky, Rotating black holes: Separable wave equations for gravitational and electromagnetic perturbations, *Phys. Rev. Lett.* **29**, 1114 (1972).
- [38] S. A. Teukolsky, Perturbations of a Rotating Black Hole. I. Fundamental Equations for Gravitational, Electromagnetic, and Neutrino-Field Perturbations, *Astrophys. J.* **185**, 635 (1973).
- [39] J. D. Bekenstein, Black holes and entropy, *Phys. Rev. D* **7**, 2333 (1973).
- [40] D. Christodoulou, Reversible and irreversible transformations in black-hole physics, *Phys. Rev. Lett.* **25**, 1596 (1970).
- [41] S. W. Hawking, Gravitational radiation from colliding black holes, *Phys. Rev. Lett.* **26**, 1344 (1971).
- [42] S. Hod, Bohr’s correspondence principle and the area spectrum of quantum black holes, *Phys. Rev. Lett.* **81**, 4293 (1998), [arXiv:gr-qc/9812002](#).
- [43] A. Coates, S. H. Völkel, and K. D. Kokkotas, Spectral Lines of Quantized, Spinning Black Holes and their Astrophysical Relevance, *Phys. Rev. Lett.* **123**, 171104 (2019), [arXiv:1909.01254 \[gr-qc\]](#).
- [44] S. Datta and K. S. Phukon, Imprint of black hole area quantization and Hawking radiation on inspiraling binary, *Phys. Rev. D* **104**, 124062 (2021), [arXiv:2105.11140 \[gr-qc\]](#).
- [45] V. Cardoso, M. Cavaglia, and L. Gualtieri, Hawking emission of gravitons in higher dimensions: Non-rotating black holes, *JHEP* **02**, 021, [arXiv:hep-th/0512116](#).
- [46] E. Berti, V. Cardoso, and A. O. Starinets, Quasinormal modes of black holes and black branes, *Class. Quant. Grav.* **26**, 163001 (2009), [arXiv:0905.2975 \[gr-qc\]](#).
- [47] T. M. MacRobert, Higher transcendental functions, *Nature* **175**, 317 (1955).
- [48] R.-Z. Guo, C. Yuan, and Q.-G. Huang, Near-horizon microstructure and superradiant instabilities of black holes, *Phys. Rev. D* **105**, 064029 (2022), [arXiv:2109.03376 \[gr-qc\]](#).
- [49] J. a. G. Rosa and T. W. Kephart, Stimulated Axion Decay in Superradiant Clouds around Primordial Black Holes, *Phys. Rev. Lett.* **120**, 231102 (2018), [arXiv:1709.06581 \[gr-qc\]](#).
- [50] L. Chen, D. Huang, and C.-Q. Geng, Effects of stimulated emission and superradiant growth of non-spherical axion cluster, (2023), [arXiv:2311.01819 \[hep-ph\]](#).
- [51] R.-Z. Guo, C. Yuan, and Q.-G. Huang, On the interaction between ultralight bosons and quantum-corrected black holes, *JCAP* **04**, 069, [arXiv:2301.06840 \[gr-qc\]](#).
- [52] Y. Cao and Y. Tang, Signatures of ultralight bosons in compact binary inspiral and outspiral, *Phys. Rev. D* **108**, 123017 (2023), [arXiv:2307.05181 \[gr-qc\]](#).